E7-2026-3

A. V. Isaev [1,2,*], R. S. Mukhin [1], A. V. Andreev [1,2],
A. Rahmatinejad [1,2], T. M. Shneidman [1,2], V. I. Chepigin [1],
V. D. Danilkin [1], H. M. Devaraja [1,2], A. Ismailova [1,2],
I. N. Izosimov [1], A. A. Kuznetsova [1], O. N. Malyshev [1],
Yu. A. Popov [1], B. Sailaubekov [1,2,3], E. A. Sokol [1],
M. S. Tezekbayeva [1,2], I. I. Ulanova [1], A. I. Svirikhin [1,2]

PROMPT NEUTRON EMISSION IN THE SPONTANEOUS FISSION OF ^{258,260}Sg

Submitted to "Physical Review C"

[1] Joint Institute for Nuclear Research, Dubna 141980, Russia
[2] Institute of Nuclear Physics, Almaty 050032, Kazakhstan
[3] L. N. Gumilyov Eurasian National University,
Astana 010000, Kazakhstan
* E-mail: isaev@jinr.ru

Исаев А. В. и др. E7-2026-3

Эмиссия мгновенных нейтронов в спонтанном делении ^{258,260}Sg

Исследование свойств распада изотопов ^{258,260}Sg, образующихся в реакциях полного слияния ^{207}Pb + ^{52,54}Cr, было выполнено с использованием фильтра скоростей SHELS. Множественности мгновенных нейтронов при спонтанном делении ^{258,260}Sg были измерены впервые. Средние числа нейтронов в актах деления составили $\overline{\nu}(^{258}\mathrm{Sg}) = 4{,}9 \pm 0{,}4$ и $\overline{\nu}(^{260}\mathrm{Sg}) = 5{,}03 \pm 0{,}14$. Коэффициент ветвления по пути α-распада изотопа ^{260}Sg был определен как $b_\alpha = 0{,}29 \pm 0{,}03$. Периоды полураспада были измерены при доверительном интервале 95 %: $T_{1/2}(^{258}\mathrm{Sg}) = 2{,}2^{+2,4}_{-1,0}$ мс и $T_{1/2}(^{260}\mathrm{Sg}) = 7{,}0^{+2,6}_{-1,7}$ мс.

Работа выполнена в Лаборатории ядерных реакций им. Г. Н. Флерова ОИЯИ.

Препринт Объединенного института ядерных исследований. Дубна, 2026

Isaev A. V. et al. E7-2026-3

Prompt Neutron Emission in the Spontaneous Fission of ^{258,260}Sg

An experimental study of ^{258,260}Sg produced in the complete fusion reactions ^{207}Pb + ^{52,54}Cr was performed using the SHELS velocity filter. Prompt neutron multiplicities in the spontaneous fission of ^{258,260}Sg were measured for the first time, yielding average values of $\overline{\nu}(^{258}\mathrm{Sg}) = 4.9 \pm 0.4$ and $\overline{\nu}(^{260}\mathrm{Sg}) = 5.03 \pm 0.14$. The α-decay branching ratio of ^{260}Sg was determined to be $b_\alpha = 0.29 \pm 0.03$. In addition, the half-lives were measured as $T_{1/2}(^{258}\mathrm{Sg}) = 2.2^{+2.4}_{-1.0}$ ms (95% C.L., confidence limit) and $T_{1/2}(^{260}\mathrm{Sg}) = 7.0^{+2.6}_{-1.7}$ ms (95% C.L.).

The investigation has been performed at the Flerov Laboratory of Nuclear Reactions, JINR.

Preprint of the Joint Institute for Nuclear Research. Dubna, 2026

INTRODUCTION

The study of spontaneous fission (SF) of superheavy elements (SHE) remains a major challenge in nuclear physics, as experimental data are scarce, despite the process becoming increasingly important for these nuclei. In particular, fission data are practically absent even for seaborgium isotopes ($Z = 106$). Crucial characteristics remain unknown, including the total kinetic energy and mass distributions of the fragments, as well as the yields of prompt neutrons and γ rays.

The region near the neutron number $N = 152$ is of particular interest due to enhanced shell stabilization, which is expected to affect fission barriers and the evolution of the fission process. Recent experimental studies of neutron-deficient Sg isotopes, including new data on ^{257}Sg [1], indicate that shell effects in this region may significantly influence SF dynamics. This work addresses this gap by providing the first information on the yields of prompt neutrons from the SF of the neutron-deficient isotopes ^{258,260}Sg, which lie near the closed neutron subshell $N = 152$.

Prompt neutron data can shed light on the SF dynamics and provide a reliable basis for the development of advanced fission models for SHE at the boundaries of nucleonic stability. Furthermore, as shown in our previous study of the SF of ^{256}Rf [2], prompt neutron multiplicity distributions can, in certain cases, be useful for identifying different fission modes in SHE.

1. EXPERIMENTAL DETAILS

An experiment aimed at studying the SF properties of ^{258,260}Sg was performed at FLNR using the SHELS separator [3] and the SFiNx detection system [4] (Fig. 1). For the present study, the data were collected in three experimental runs. The detection system includes 116 ^{3}He neutron counters capable of detecting multiple prompt neutrons emitted during the SF process, as well as a "well-like" assembly of double-sided silicon detectors (DSSD), consisting of a 128×128-strip focal-plane detector and eight tunnel detectors with 16×16 strips each, used to register fission fragments and α particles. The DSSD energy calibration for α particles was carried out using the $^{154}\mathrm{Sm}(^{52,\,54}\mathrm{Cr}, xn)^{206-x,\,208-x}\mathrm{Rn}$ reactions. The detection efficiency of the focal-plane silicon detector is approximately 50% for α particles and nearly 100% for at least one of the two fission fragments.

Before implantation into the focal-plane DSSD, evaporation residues traversed the foils of the time-of-flight (ToF) system [5], which was used

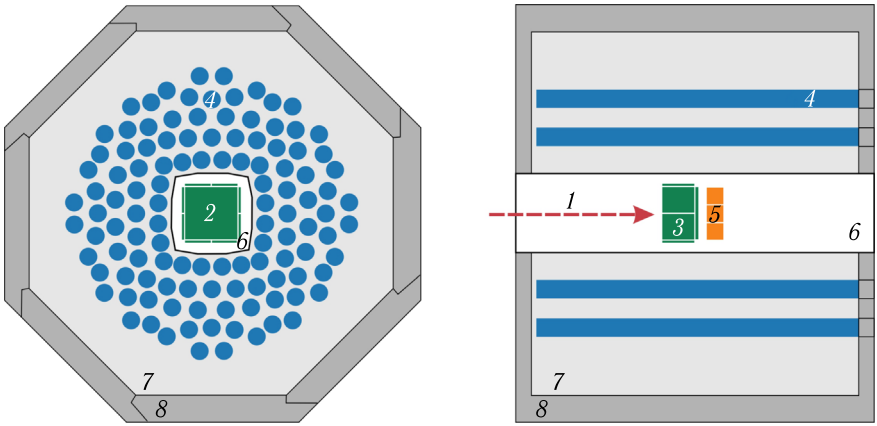

Fig. 1. Schematic view of the SFiNx detection system: front view (left) and side view (right). Legend: *1* — recoil nuclei; *2* — focal-plane Si detector; *3* — tunnel Si detectors; *4* — ^{3}He counters; *5* — CLLBC scintillation detectors; *6* — vacuum chamber; *7* — moderator; *8* — shield to reduce background

to distinguish implantation events from subsequent decays registered in the focal-plane detector. Additionally, a thin Mylar foil was placed directly in front of the entrance to the DSSD "well" assembly to suppress soft background originating from parasitic reaction products and scattered beam ions. Passage through the ToF foils and the Mylar degrader resulted in a reduction of the measured recoil energies in DSSD; this effect is taken into account in the correlation analysis described below.

The single neutron detection efficiency, calibrated with a ^{248}Cm source, was approximately 56% (see below for experiment-specific values), and the average neutron lifetime in the detector array was (19 ± 1) μs. The high granularity of the SFiNx neutron detector minimizes the probability that more than one neutron is registered in a single ^{3}He counter within the coincidence window [4].

Nine CLLBC-based scintillator detectors were installed directly after the focal-plane DSSD for the registration of prompt γ rays. The SFiNx detector system was situated behind a wall of heavy concrete about 2 m thick to reduce neutron and gamma backgrounds.

The isotope ^{260}Sg was synthesized in the complete-fusion reaction of ^{54}Cr ions from the U-400 cyclotron with a ^{207}PbS target. Two PbS targets with thicknesses of 345 and 455 μg/cm^2 (^{207}Pb enrichment around 99.4%) were electrochemically deposited on 1.5 μm-thick Ti backing foils. Measurements were carried out at beam energies at the center of the target ($E_{1/2}$), spanning 251–255 MeV for the 345 μg/cm^2 target and 249–254 MeV for the 455 μg/cm^2 target. The ^{54}Cr mean equilibrium charge state after passing through a thin C-foil was calculated using the semi-empirical formula [6],

yielding $\langle q \rangle = +21$. The total number of projectiles delivered to the targets and measured in a Faraday cup was approximately $3.6 \cdot 10^{18}$.

The ^{258}Sg isotope was obtained in a complete-fusion reaction induced by ^{52}Cr ions from the cyclotron on a ^{207}PbS target. A 455 μg/cm^2 PbS target, prepared as described above, was used. Due to the absence of experimental cross-section data for the reaction under study, the beam energies ($E_{1/2}$) were selected in the range 249–253 MeV by extrapolating values from related ^{52}Cr-induced reactions [1, 7]. The total number of beam ions transmitted through the target was approximately $1.4 \cdot 10^{18}$. The corresponding mean equilibrium charge state of the ^{52}Cr ions was also $\langle q \rangle = +21$.

2. RESULTS

2.1. Decay of ^{260}Sg. Spontaneous-fission events following the implantation of evaporation residues were searched for within a 0–50 ms time window. Recoil energies were restricted to 11–30 MeV, and fission fragments were required to have energies above 20 MeV. Applying these criteria yielded 290 recoil–SF correlations.

A fraction of these events originates from the α decay of ^{260}Sg to ^{256}Rf, which also undergoes spontaneous fission. Since the lifetimes of ^{260}Sg ($(4.95 \pm \pm 0.33)$ ms [8]) and ^{256}Rf ((6.2 ± 0.2) ms [9]) are similar, timing information alone does not allow their separation.

To suppress the contribution of ^{256}Rf, a search for recoil–α–SF correlations was performed. The α-particle search was carried out over a wide energy interval of 8–11 MeV. The observed α-particle energies (Fig. 2)

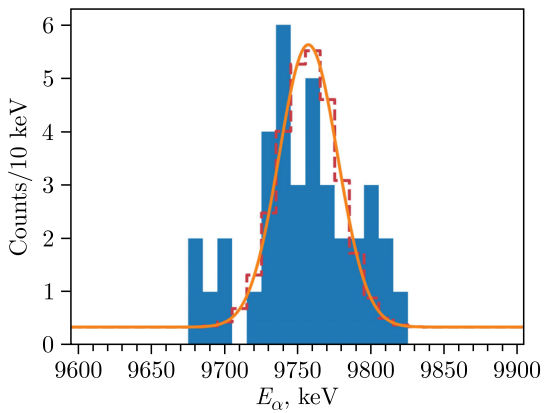

Fig. 2. Spectrum of α particles of ^{260}Sg obtained via recoil–α–SF correlations in the focal-plane detector. The blue bars represent the experimental data. The solid orange curve displays a continuous fit using a Gaussian peak with a fixed 20 keV detector resolution and constant background, fitted using Poisson-binned maximum likelihood as recommended in [14]. The red dashed curve shows the expected counts per bin from the fitted model

are concentrated at the known α-decay line of ^{260}Sg, providing a reliable identification. Events containing such α signals were rejected. This procedure removed 59 SF events (based on 42 α from the focal-plane detector and 17 α from the side detectors), resulting in a final data set of 231 SF events. As α particles emitted into the backward hemisphere are not always detected, the rejection is not complete. Consequently, the final SF event sample is estimated to contain a (11 ± 2)% residual admixture of ^{256}Rf.

The α-decay branching ratio of ^{260}Sg was determined to be $b_\alpha = 0.29 \pm \pm 0.03$, consistent with previous values $b_\alpha = 0.29 \pm 0.03$ [8], $b_{\mathrm{SF}} = 0.77 \pm \pm 0.09$ [10], $b_\alpha = 0.5^{+0.2}_{-0.3}$ [11] and inconsistent with the earlier estimates $b_\alpha > 0.8$ reported in [12, 13] (which were based on limited statistics).

The α-particle peak was fitted following the procedure of [14]. The peak centroid, (9757 ± 6) keV, agrees with the reported value of (9748 ± 1) keV [8, 15]. Due to limited statistics, no conclusions can be drawn regarding the additional line at (9715 ± 3) keV reported in [8, 15].

The half-life of ^{260}Sg was determined using two independent methods. Using the method of [16], applied to lifetime data from recoil–SF correlations (Fig. 3), a value of $T_{1/2} = (6.5 \pm 0.3)$ ms was obtained. An independent analysis based on recoil–α–SF correlations was performed using a maximum-likelihood estimator applied to the decay-time distribution. This approach yielded $T_{1/2} = 7.0^{+2.6}_{-1.7}$ ms (95% C.L.), with the confidence limits obtained from the exact likelihood-ratio method. The two results are statistically compatible within their uncertainties and demonstrate consistency between the applied analysis methods.

The statistical test of [16] shows no statistically significant evidence for additional decay components in the lifetime distributions owing to the limited

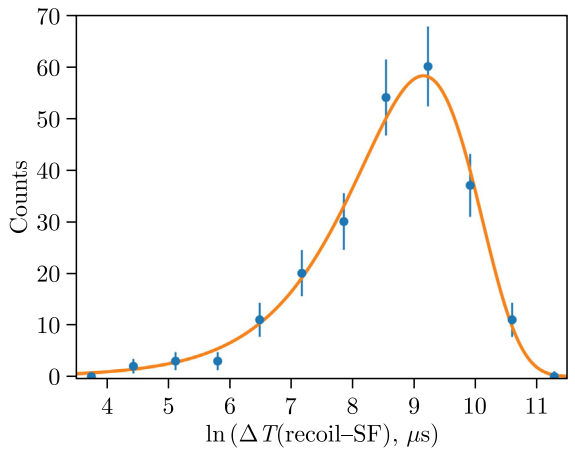

Fig. 3. Distribution of time differences between recoil nuclei implantation and fission-fragment detections for ^{260}Sg. The blue points represent the experimental data. The orange solid curve shows the exponential fit

number of decay events. While most recoil–α correlations are consistent with a half-life of about 5 ms, a small number of longer-lived events is observed, leading to a longer half-life. This behavior is attributed to the limited statistics and to the possible presence of unresolved α-decay fine structure previously reported for ^{260}Sg [8, 15].

The obtained half-life value $7.0^{+2.6}_{-1.7}$ ms is consistent with earlier measurements for ground-state decay (4.95 ± 0.33) ms [8, 15], $3.6^{+0.9}_{-0.6}$ ms [11], $3.0^{+0.7}_{-0.5}$ ms [10]. It is also consistent with a longer-lived activity of $6.7^{+9.1}_{-2.5}$ ms reported in [10].

The half-life of ^{256}Rf was found to be $T_{1/2} = 5.3^{+2.0}_{-1.3}$ ms (95% C.L.) using the same recoil–α–SF correlations. This is consistent with previous values (6.2 ± 0.2) ms [9], (6.7 ± 0.2) ms [2], (6.7 ± 0.2) ms [17], (6.9 ± 0.4) ms [18], and (6.9 ± 0.2) ms [19]. No α decay of ^{256}Rf was observed in this experiment.

Prompt neutrons emitted in SF were searched for in the time interval 0–128 μs after the fission-fragment signal in the focal-plane DSSD. This choice is based on the average neutron lifetime of (19 ± 1) μs in the setup. A total of 645 prompt neutrons in coincidence with 231 fission events attributed to ^{260}Sg were registered. These data (Table 1) represent the first measurement of prompt-neutron emission from ^{260}Sg. After correction for the neutron detection efficiency (55.5 ± 1.0)%, the neutron emission distribution yields an average multiplicity of $\overline{\nu} = 5.03 \pm 0.14$.

The Tikhonov regularization method [20, 21] was applied to reconstruct the true neutron emission probabilities from the measured neutron multiplicity distribution. The resulting reconstructed distribution is shown in Fig. 4.

Background neutrons were studied by analyzing 1000 time windows of length 128 μs starting at 1000 μs from each fission event. The start time of these background search gates (1000 μs) was selected to minimize overlap with prompt neutrons. The resulting background distribution (Table 1) was

Table 1. **Observed number of SF events (N) and background neutron probabilities (b_ν), categorized by the number of detected neutrons, together with the reconstructed neutron emission probabilities (P_ν) for ^{260}Sg**

ν	N	b_ν	P_ν
0	10	0.997	0.002 ± 0.004
1	36	0.003	0.025 ± 0.010
2	55	$2 \cdot 10^{-5}$	0.058 ± 0.013
3	60	0	0.107 ± 0.015
4	41	0	0.163 ± 0.017
5	22	0	0.208 ± 0.020
6	6	0	0.214 ± 0.018
7	0	0	0.157 ± 0.013
8	0	0	0.063 ± 0.019
9	1	0	$0.003^{+0.005}_{-0.003}$
10	0	0	< 0.006

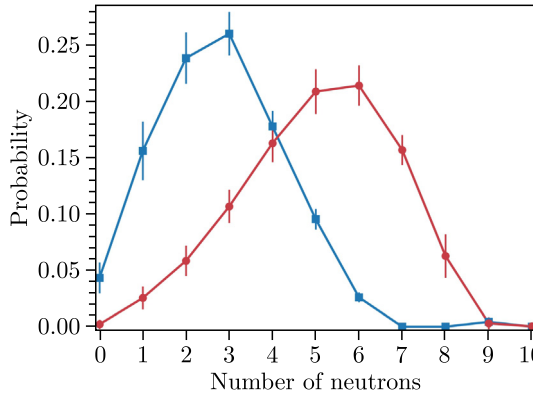

Fig. 4. Neutron multiplicity distributions for the SF of ^{260}Sg: measured distribution (blue squares) and reconstructed distribution (red circles)

used in the correction procedure. The average background multiplicity was 0.003 neutrons per fission and has a negligible effect on the prompt neutron multiplicity distribution.

The average number of prompt neutrons in the SF of ^{256}Rf, deduced from the same recoil–α–SF correlations, is 4.7 ± 0.2, consistent with the previously reported value of 4.30 ± 0.17 [2].

2.2. Decay of ^{258}Sg. A total of nine SF events of ^{258}Sg were identified. The search was performed within a 0–50 ms time window following implantation signals of recoils searched for over a broad energy range of 2–50 MeV. All recoils associated with SF events were found to have energies between 11 and 17 MeV. The energy of the fission fragments was required to exceed 20 MeV. Spontaneous-fission events were accepted only if accompanied by either a coincident signal from a second fragment in the side detectors or prompt γ rays in the scintillation detectors.

Table 2. **Observed number of SF events (N) for ^{258}Sg and background neutron probabilities (b_ν), categorized by the number of detected neutrons**

ν	N	b_ν
0	0	0.995
1	1	0.005
2	3	$3 \cdot 10^{-5}$
3	3	0
4	1	0
5	1	0

Prompt neutrons were searched for in the time interval 0–128 μs after the fission signal in the focal-plane Si detector. A total of 25 prompt neutrons in coincidence with nine fission events attributed to ^{258}Sg were registered. The distribution of the nine recorded fission events as a function of neutron multiplicity ν is given in Table 2.

After correction for the neutron detection efficiency $(56.8 \pm 1.0)\%$, the neutron emission distribution yields an average multiplicity of $\overline{\nu} = 4.9 \pm 0.4$. Compared to the previous experiment, a slight increase in single neutron detection efficiency (from $(55.5 \pm 1.0)\%$ to $(56.8 \pm 1.0)\%$) was achieved.

This improvement results from the unification of most ^{3}He counters, which facilitated optimal adjustment of the discriminator thresholds.

Background neutrons were studied using the method described above for ^{260}Sg. The total number of time windows analyzed from each SF event was 10 000, yielding an average background multiplicity of 0.006 neutrons per fission (Table 2).

The half-life of ^{258}Sg was determined as $T_{1/2} = 2.2^{+2.4}_{-1.0}$ ms (95% C.L.) using a maximum-likelihood estimator applied to lifetimes from the recoil–SF correlations. The obtained half-life value agrees with previously reported data $2.1^{+1.0}_{-0.6}$ ms [7], $2.7^{+0.9}_{-0.7}$ ms [22], and $2.9^{+1.3}_{-0.7}$ ms [9].

To reliably detect the α decay of ^{258}Sg, we searched for recoil–α–SF and recoil–α–α correlations, taking into account $b_{\alpha}(^{254}\mathrm{Rf}) \leqslant 0.015$ [9]. An α-search interval of 0–50 ms was applied after the recoil implantation signal, and a 0–10 ms fission or second α-decay search interval followed the first α detection. For this analysis, only α particles with energies of 7–11 MeV were accepted. Consequently, no α-decay events were observed.

3. DISCUSSION

The systematic behavior of the average prompt neutron multiplicity as a function of the parameter $Z^2/A^{1/3}$ for nuclides with $Z = 92$–106 is shown in Fig. 5. The present values for ^{258,260}Sg follow the general increasing trend with fissility and agree with expectations for SHE.

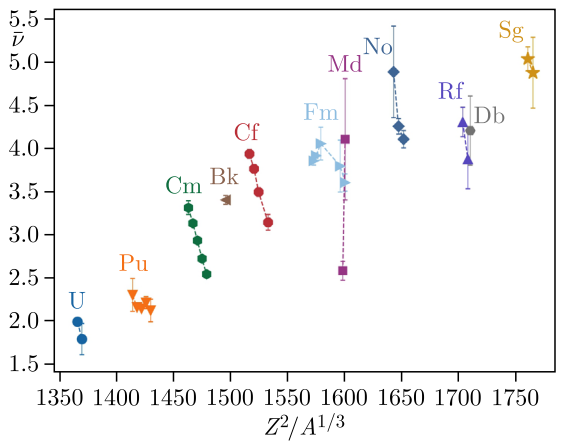

Fig. 5. Average prompt neutron multiplicity vs. the parameter $Z^2/A^{1/3}$ for the SF of nuclides with $Z = 92$–106. References: U — [23, 24]; Pu — [25–27]; Cm — [25, 28]; Bk — [28]; Cf — [25, 26, 28, 29]; Fm — [29–33]; Md — [34, 35]; No — [4, 36, 37]; Rf — [2, 38]; Db — [39]; Sg — this work. For ^{268}Db, $\overline{\nu} = 4.2 \pm 0.4$; the uncertainty was estimated in this work since the original reference [39] does not provide it

The calculation of the neutron multiplicity distribution in the SF of ^{260}Sg is presented in Fig. 6. The calculations were performed within the improved scission-point model [40–43] with random walk. It is assumed that after crossing the fission barrier, the nucleus is represented as a superposition of various dinuclear systems (DNS), i. e., the system of two fragments in touching. The DNS fragments evolve by stretching and exchanging nucleons. This evolution is treated in competition with the decay of DNS into two hot primary fission fragments. The de-excitation of fission fragments through neutron emission is treated using Monte Carlo simulations, taking into account the distribution of kinetic energy of neutrons [44]. The parameters of the model are fixed by fitting the average neutron multiplicities in the SF of ^{252}No [4], ^{256}Rf [2], ^{260}Md [34], and ^{258,260}Sg (current work). The model is presented in detail in [42, 43], and its application to the description of neutron multiplicities of ^{256}Rf is given in [2]. It is worth mentioning that in comparison to the calculations in [2], in the current version of the model, level densities were calculated in the microscopical approach, taking into account both pairing and shell effects at each given deformations of DNS fragments.

As seen in Fig. 6, the results of the calculations are in excellent agreement with the experimental data. Compared to ^{256}Rf [2], the neutron multiplicity for the SF of ^{260}Sg shows a less pronounced tail toward small neutron multiplicities ν; instead, it has a wide and more uniform distribution with considerable probabilities for fission events with small ν. To analyze the

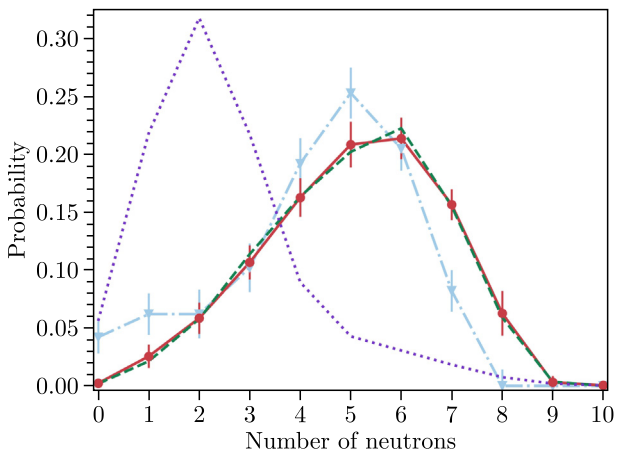

Fig. 6. Prompt neutron emission probability distributions for ^{260}Sg: the experimental distribution obtained in this work (red circles) and theoretical predictions from the improved scission-point model [40–43] (green dashed curve) and GEF model [45] (violet dotted curve). For comparison, the prompt neutron multiplicity distribution of ^{256}Rf from work [2] (cyan triangles) is also included

mass splits that are responsible for fission events, the partial mass distributions representing contributions to the SF of ^{260}Sg with specific neutron multiplicities are shown together with the total mass distribution in Fig. 7. It is seen that the mass distribution exhibits both symmetric and asymmetric modes for $\nu \leqslant 4$ and becomes asymmetric for $5 \leqslant \nu \leqslant 7$. Interestingly, for

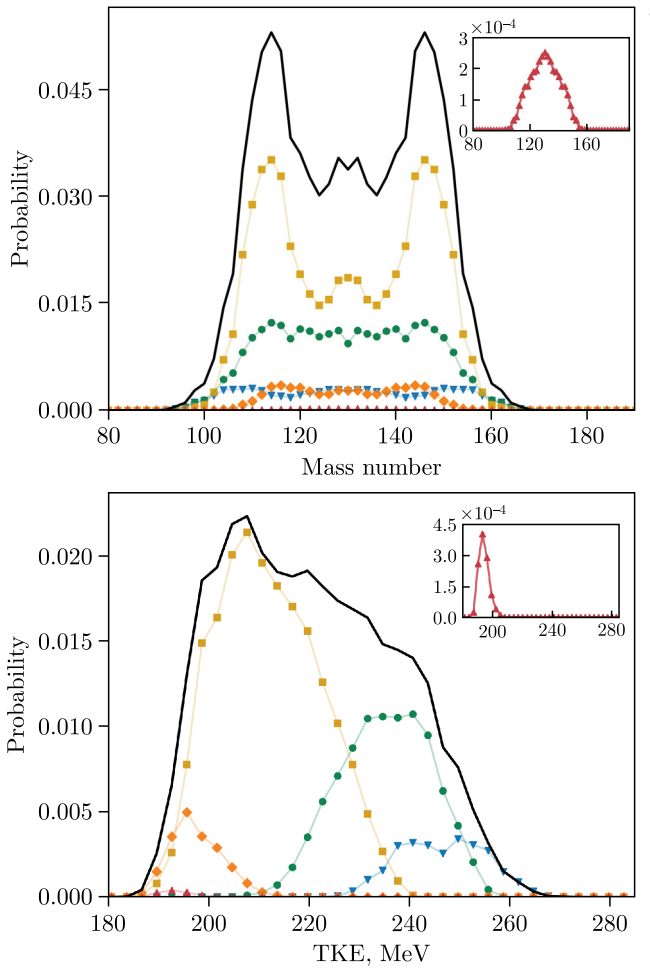

Fig. 7. Calculated mass distributions of fission fragments (*a*) and total kinetic energy (TKE) distributions of the fragments (*b*) for ^{260}Sg spontaneous fission. The results are categorized by prompt neutron multiplicity (ν): the solid black line represents the total distribution summed over all multiplicities; blue triangles down denote $0 \leqslant \nu \leqslant 2$; green circles — $3 \leqslant \nu \leqslant 4$; yellow squares — $5 \leqslant \nu \leqslant 7$; orange diamonds — $\nu = 8$, and red triangles — up $9 \leqslant \nu \leqslant 10$ (see inset)

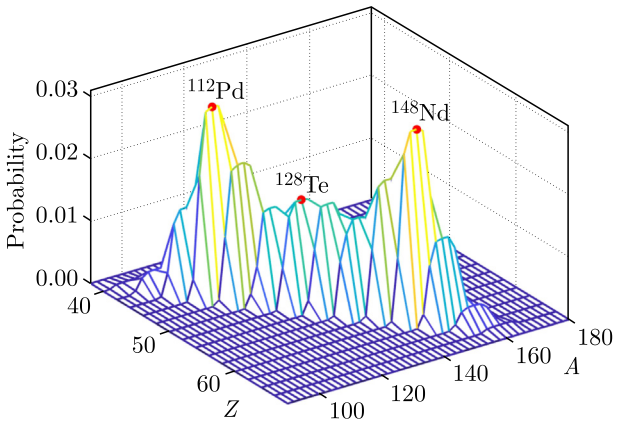

Fig. 8. Calculated mass-charge distribution for the SF of ^{260}Sg. Fission fragments corresponding to the most probable symmetric ^{128}Te + ^{128}Te and asymmetric ^{112}Pd + ^{148}Nd splits are indicated

even larger values of ν, the mass distribution again starts to evolve toward a symmetric one and becomes fully symmetric for $9 \leqslant \nu \leqslant 10$. This mode corresponds to the same scission configurations as $\nu \leqslant 2$ but with strongly deformed fragments that is revealed by small TKE values (see inset panels in Fig. 7).

The role of various scission configurations is elucidated in Fig. 8 where the mass-charge distribution is presented. The maximum of the asymmetric mass split corresponds to the dinuclear system ^{112}Pd + ^{148}Nd with soft fragments that are strongly deformed before DNS decay. Upon decay, the energy stored as the deformations of fragments is released as excitation energy leading to a large neutron multiplicity. On the contrary, the symmetric split corresponds to the fragments ^{128}Te + ^{128}Te which are relatively stiff against deformation. As a result, the dinuclear system composed of these fragments decays from compact shapes leading to the fission events with few or no emitted neutrons and a correspondingly high TKE, as demonstrated in Fig. 7. With very small probabilities, this scission configuration can become strongly deformed, leading to fission events with a large $\nu \geqslant 8$ and small TKE values.

The average number of neutrons emitted in SF was calculated as $\overline{\nu}(^{258}\mathrm{Sg}) = 4.99$ and $\overline{\nu}(^{260}\mathrm{Sg}) = 5.07$. These values agree well with the experimental data.

We also compared our results with the GEF model [45] (version 2025/1.2). The model was found to significantly underestimate the $\overline{\nu}$ value and fails to describe the shape of the prompt neutron multiplicity distribution (see Fig. 6).

CONCLUSIONS

For the first time, the prompt-neutron emission probabilities for different neutron multiplicities were measured for the SF of ^{258,260}Sg. The average neutron multiplicities were determined to be $\overline{\nu}(^{258}\mathrm{Sg}) = 4.9 \pm 0.4$ and $\overline{\nu}(^{260}\mathrm{Sg}) = 5.03 \pm 0.14$.

In addition, the half-lives $T_{1/2}(^{258}\mathrm{Sg}) = 2.2^{+2.4}_{-1.0}$ ms (95% C.L.) and $T_{1/2}(^{260}\mathrm{Sg}) = 7.0^{+2.6}_{-1.7}$ ms (95% C.L.), as well as the α-decay branching ratio $b_\alpha(^{260}\mathrm{Sg}) = 0.29 \pm 0.03$, were obtained. All of these values are consistent with previous measurements.

A comparison with the calculations based on the improved scission-point model shows good agreement with the experimental data, reproducing both the average neutron multiplicity and the shape of the multiplicity distribution for ^{260}Sg, as well as the average multiplicity for ^{258}Sg. This indicates that the model provides an adequate description of spontaneous fission properties in these superheavy nuclei.

These new results on neutron multiplicities in the spontaneous fission of neutron-deficient seaborgium isotopes provide an important benchmark for fission theory in the superheavy-element region and demonstrate the influence of shell structure on fission observables. They also lay the groundwork for future prompt-neutron studies in neighboring superheavy nuclei, which will further elucidate the fission process at the limits of nuclear stability.

Funding. This research has been funded by the Committee of Science of the Ministry of Science and Higher Education of the Republic of Kazakhstan (Grant No. BR28712431).

Acknowledgements. The authors express their deep gratitude to Dr. A. G. Popeko for comprehensive assistance in conducting the experiments, to the U-400 cyclotron and ion source teams for providing high-quality ^{52,54}Cr beams, and to the FLNR Transactinide Chemistry Sector staff for manufacturing chromocene and accelerator targets.

Appendix.
AUXILIARY ESTIMATES OF PRODUCTION CROSS SECTIONS FOR ^{258,260}Sg

This Appendix presents auxiliary estimates of production cross sections for the $1n$ evaporation channel in the $^{207}\mathrm{Pb} + ^{52,54}\mathrm{Cr}$ reactions. These estimates were not used in the analysis or interpretation of the prompt-neutron emission data discussed in the main text and do not affect the conclusions of the paper. The values are provided solely for completeness and for comparison with previously reported systematics and should be regarded as indicative rather than precise. The estimates are shown in Fig. 9.

For the reaction $^{207}\mathrm{Pb}(^{54}\mathrm{Cr}, 1n)^{260}\mathrm{Sg}$, the estimated values are consistent, within uncertainties, with previously reported data [15]. For the reaction

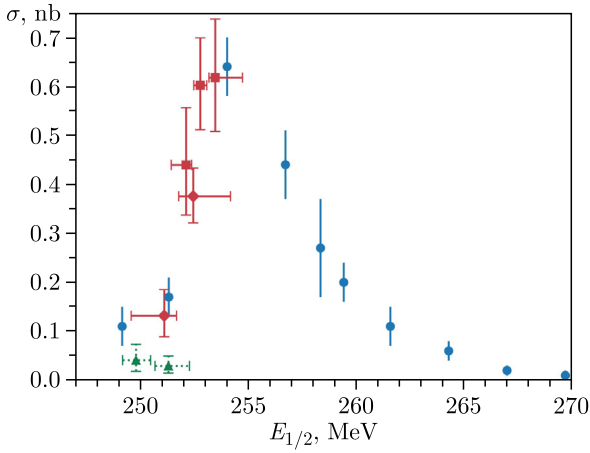

Fig. 9. Production cross sections for the ^{207}Pb(^{54}Cr, $1n$)^{260}Sg reaction from [15] (blue circles) and estimates from the present work (red squares for the 345 μg/cm^2 target and red diamonds for the 455 μg/cm^2 target). Estimates for the ^{207}Pb(^{52}Cr, $1n$)^{258}Sg reaction from the present work are shown by green triangles. The beam energy is given after passing through half of the target thickness. The presented values are provided for comparison only

^{207}Pb(^{52}Cr, $1n$)^{258}Sg, no experimental cross-section data have been reported previously. The nuclide ^{258}Sg has been synthesized earlier in the reactions ^{208}Pb(^{52}Cr, $2n$)^{258}Sg [1, 7] and ^{209}Bi(^{51}V, $2n$)^{258}Sg [9, 22].

REFERENCES

1. *Mosat P. et al.* Probing the Shell Effects on Fission: The New Superheavy Nucleus ^{257}Sg // Phys. Rev. Lett. 2025. V. 134, No. 23. P. 232501; https://doi.org/10.1103/s7hr-y7zq.
2. *Isaev A. V. et al.* Structure of the Prompt Neutron Multiplicity Distribution in the Spontaneous Fission of ^{256}Rf // Phys. Lett. B. 2023. V. 843. P. 138008; https://doi.org/10.1016/j.physletb.2023.138008.
3. *Popeko A. G. et al.* Separator for Heavy ELement Spectroscopy — Velocity Filter SHELS // Nucl. Instr. Meth. B. 2016. V. 376. P. 140–143; doi: 10.1016/j.nimb.2016.03.045.
4. *Isaev A. V. et al.* The SFiNx Detector System // Phys. Part. Nucl. Lett. 2022. V. 19, No. 1. P. 37–45; doi: 10.1134/s154747712201006x.
5. *Andreyev A. N. et al.* Large Area High-Efficiency Time-of-Flight System for Detection of Low Energy Heavy Evaporation Residues at the Electrostatic Separator VASSILISSA // Nucl. Instr. Meth. A. 1995. V. 364, No. 2. P. 342–348; https://doi.org/10.1016/0168-9002(95)00355-X.
6. *Shima K., Ishihara T., Utsumi H.* Charge States of Ions Passing through Thin Films // Nucl. Instr. Meth. 1982. V. 200, No. 2–3. P. 605–608.

7. *Folden C. M. III et al.* Measurement of the ^{208}Pb(^{52}Cr, n)^{259}Sg Excitation Function // Phys. Rev. C. 2009. V. 79, No. 2. P. 027602; doi: 10.1103/PhysRevC.79.027602.
8. *Heßberger F. P. et al.* Decay Properties of Neutron-Deficient Isotopes of Elements from $Z = 101$ to $Z = 108$ // Eur. Phys. J. A. 2009. V. 41, No. 2. P. 145–153; doi: 10.1140/epja/i2009-10826-2.
9. *Heßberger F. P. et al.* Spontaneous Fission and Alpha-Decay Properties of Neutron Deficient Isotopes $^{257-253}$104 and ^{258}106 // Z. Phys. A: Hadrons Nucl. 1997. V. 359, No. 4. P. 415–425; doi: 10.1007/s002180050422.
10. *Streicher B.* Synthesis and Spectroscopic Properties of Transfermium Isotopes with $Z = 105$, 106 and 107. PhD thesis. Comenius University, Bratislava, 2006.
11. *Münzenberg G. et al.* The Isotopes ^{259}106, ^{260}106, and ^{261}106 // Z. Phys. A. 1985. V. 322, No. 2. P. 227–235; doi: 10.1007/bf01411887.
12. *Demin A. G. et al.* On the Properties of the Element 106 Isotopes Produced in the Reactions Pb + ^{54}Cr // Z. Phys. A. 1984. V. 315, No. 2. P. 197–200; doi: 10.1007/bf01419379.
13. *Oganessian Yu. Ts. et al.* Experimental Studies of the Formation and Radioactive Decay of Isotopes with $Z = 104-109$ // Radiochimica Acta. 1984. V. 37, No. 3. P. 113–120; doi: 10.1524/ract.1984.37.3.113.
14. *García-Toraño E.* Fitting of Low-Statistics Peaks in Alpha-Particle Spectra // Nucl. Instr. Meth. A. 1994. V. 339, No. 1. P. 122–126; https://doi.org/10.1016/0168-9002(94)91790-6.
15. *Sulignano B.* Search for K Isomers in ^{252,254}No and ^{260}Sg and Investigation of Their Nuclear Structure. PhD thesis. Johannes Gutenberg University, Mainz, 2007.
16. *Schmidt K. H.* A New Test for Random Events of an Exponential Distribution // Eur. Phys. J. A. 2000. V. 8, No. 1. P. 141–145; doi: 10.1007/s100500070129.
17. *Oganessian Yu. Ts. et al.* On the Stability of the Nuclei of Element 108 with $A = 263-265$ // Z. Phys. A. 1984. V. 319. P. 215–217; doi: 10.1007/bf01415635.
18. *Robinson A. P. et al.* Search for a 2-Quasiparticle High-K Isomer in ^{256}Rf // Phys. Rev. C. 2011. V. 83, No. 6. P. 064311; doi: 10.1103/PhysRevC.83.064311.
19. *Greenlees P. T. et al.* Shell-Structure and Pairing Interaction in Superheavy Nuclei: Rotational Properties of the $Z = 104$ Nucleus ^{256}Rf // Phys. Rev. Lett. 2012. V. 109, No. 1. P. 012501; doi: 10.1103/PhysRevLett.109.012501.
20. *Turchin V. F., Kozlov V. P., Malkevich M. S.* The Use of Mathematical-Statistics Methods in the Solution of Incorrectly Posed Problems // Sov. Phys. Usp. 1971. V. 13, No. 6. P. 681–703; doi: 10.1070/pu1971v013n06abeh004273.
21. *Mukhin R. S. et al.* Reconstruction of Spontaneous Fission Neutron Multiplicity Distribution Spectra by the Statistical Regularization Method // Phys. Part. Nucl. Lett. 2021. V. 18, No. 4. P. 439–444; doi: 10.1134/s1547477121040130.
22. *Patin J. B.* Experimental Cross Sections for Reactions of Heavy Ions and ^{208}Pb, ^{209}Bi, ^{238}U, and ^{248}Cm Targets. PhD thesis. University of California, Berkeley, 2002.
23. *Popeko A. G. et al.* Multiplicity of Prompt Neutrons in Spontaneous Fission of ^{238}U // Sov. J. Nucl. Phys. 1976. V. 24, No. 3. P. 245–247.
24. *Belenkii S. N., Skorokhvatov M. D., Etenko A. V.* Measurement of the Characteristics of Spontaneous Fission of ^{238}U and ^{236}U // Sov. At. Energy. 1983. V. 55, No. 2. P. 528–530; doi: 10.1007/bf01138346.

25. *Orth C. J.* The Average Number of Neutrons Emitted in the Spontaneous Fission of Some Even–Even Heavy Nuclides // Nucl. Sci. Engin. 1971. V. 43, No. 1. P. 54–57; doi: 10.13182/nse71-a21245, https://doi.org/10.13182/NSE71-A21245.
26. *Lazarev Yu. A.* Variance of the Energy Distributions of Fragments Formed by Low-Energy Fission: Experimental Data and Theoretical Predictions // At. Energy Rev. 1977. V. 15, No. 1. P. 75–107.
27. *Boldeman J. W.* Prompt ν Measurements for the Spontaneous Fission of ^{240}Pu and ^{242}Pu // J. Nucl. Energy. 1968. V. 22, No. 2. P. 63–72; https://doi.org/10.1016/0022-3107(68)90055-5.
28. *Holden N. E., Zucker M. S.* Prompt Neutron Multiplicities for the Transplutonium Nuclides // Rad. Effects. 1986. V. 96, No. 1–4. P. 289–292; doi: 10.1080/00337578608211755, https://doi.org/10.1080/00337578608211755.
29. *Hoffman D. C. et al.* Neutron Multiplicity Measurements of Cf and Fm Isotopes // Phys. Rev. C. 1980. V. 21, No. 2. P. 637–646; doi: 10.1103/ PhysRevC.21.637.
30. *Sokol E. A., Zeinalov Sh. S., Ter-Akopian G. M.* Multiplicity of Fast Neutrons in the Spontaneous Fission of ^{256}Fm // Sov. At. Energy. 1989. V. 67, No. 5. P. 851–852; doi: 10.1007/bf01126141.
31. *Mukhin R. S. et al.* Prompt Neutron Multiplicity from Spontaneous Fission of ^{244}Fm // Eur. Phys. J. A. 2024. V. 60, No. 11. P. 223; doi: 10.1140/epja/s10050-024-01441-0.
32. *Choppin G. R. et al.* Prompt Neutrons from the Spontaneous Fission of Fermium-254 // Phys. Rev. 1956. V. 102, No. 3. P. 766; doi: 10.1103/PhysRev.102.766.
33. *Isaev A. V. et al.* Prompt Neutron Emission in the Spontaneous Fission of ^{246}Fm // Eur. Phys. J. A. 2022. V. 58, No. 6. P. 108; doi: 10.1140/epja/s10050-022-00761-3.
34. *Wild J. F. et al.* Prompt Neutron Emission from the Spontaneous Fission of ^{260}Md // Phys. Rev. C. 1990. V. 41, No. 2. P. 640–646; doi: 10.1103/PhysRevC.41.640.
35. *Ter-Akopyan G. M., Buklanov G. V., Zeinalov Sh. S.* Recording of Multiple Neutron Events, and a Study of Spontaneous Fission of Heavy Nuclei in Experiments on the Synthesis of Superheavy Nuclei and the Search for Them in Nature // International Workshop on the Physics of Heavy Ions. JINR Report D7-87-68. Dubna, 1987. P. 212–216 (in Russian).
36. *Mukhin R. S. et al.* Prompt Neutron Emission in ^{250}No Spontaneous Fission Associated with Ground and Isomeric State Decays // Chin. Phys. C. 2024. V. 48, No. 6. P. 064002; doi: 10.1088/1674-1137/ad361a.
37. *Isaev A. V. et al.* Comparative Study of Spontaneous-Fission Characteristics of ^{252}No and ^{254}No Isotopes // Phys. Part. Nucl. Lett. 2021. V. 18, No. 4. P. 449–456; doi: 10.1134/s1547477121040087.
38. *Svirikhin A. I. et al.* Prompt Neutrons from Spontaneous ^{254}Rf Fission // Phys. Part. Nucl. Lett. 2019. V. 16, No. 6. P. 768–771; doi: 10.1134/s1547477119060311.
39. *Oganessian Yu. Ts. et al.* Synthesis of Elements 115 and 113 in the Reaction $^{243}\mathrm{Am} + {}^{48}\mathrm{Ca}$ // Phys. Rev. C. 2005. V. 72, No. 3. P. 034611; doi: 10.1103/PhysRevC.72.034611.
40. *Andreev A. V. et al.* Possible Explanation of Fine Structures in Mass-Energy Distribution of Fission Fragments // Eur. Phys. J. A. 2004. V. 22, No. 1. P. 51–60; doi: 10.1140/epja/i2004-10017-9.
41. *Andreev A. V. et al.* Ternary Fission within Statistical Approach // Eur. Phys. J. A. 2006. V. 30, No. 3. P. 579–589; doi: 10.1140/epja/i2006-10145-2.

42. *Rahmatinejad A. et al.* Evolution of Fission Properties in Fermium Region // Intern. J. Modern Phys. E. 2024. V. 33, No. 11. P. 2441018; doi: 10.1142/s0218301324410180, https://doi.org/10.1142/S0218301324410180.
43. *Rahmatinejad A. et al.* Dependence of Angular Momentum of Fission Fragments on Total Kinetic Energy in Spontaneous Fission of ^{252}Cf // Phys. Rev. C. 2025. V. 112, No. 4. P. 044610; https://doi.org/10.1103/yklf-mh6w.
44. *Rahmatinejad A. et al.* Multi-Step Particle Emission Probabilities in Superheavy Nuclei at Moderate Excitation Energies // Phys. Lett. B. 2023. V. 844. P. 138099; https://doi.org/10.1016/j.physletb.2023.138099.
45. *Schmidt K.-H. et al.* General Description of Fission Observables: GEF Model Code // Nucl. Data Sheets. 2016. V. 131. P. 107–221; doi: 10.1016/j.nds.2015.12.009.

Received on January 27, 2026.

Редактор *В. В. Булатова*

Подписано в печать 03.03.2026.
Формат 60 × 90/16. Бумага офсетная. Печать цифровая.
Усл. печ. л. 0,93. Уч.-изд. л. 1,20. Тираж 110 экз. Заказ № 61266.

Издательский отдел Объединенного института ядерных исследований
141980, г. Дубна, Московская обл., ул. Жолио-Кюри, 6.
E-mail: publish@jinr.ru
publish.jinr.ru